

Detuning management of optical solitons in coupled quantum wells

Wen-Xing Yang,^{1,2,*} Jing-Min Hou,¹ Yuan-Yao Lin,² and Ray-Kuang Lee²

¹*Department of Physics, Southeast University, Nanjing 210096, China*

²*Institute of Photonics Technologies, National Tsing-Hua University, Hsinchu 300, Taiwan*

(Received 13 October 2008; published 17 March 2009)

We show the possibility to generate bright and dark optical solitons based on bound-to-bound intersubband transitions in an asymmetric three-coupled quantum well structure. By presenting the concept of detuning management, we show that the bright optical soliton can evolve into a dark one by adiabatically changing the corresponding one- and two-photon detunings. With adjustable carrier frequencies within the terahertz regime, we also demonstrate numerically shape-recovered collisions of two solitons in our proposed quantum wells. The present investigation may provide research opportunities in nonlinear optical experiments and may have impact on the technology for the design of semiconductor devices.

DOI: 10.1103/PhysRevA.79.033825

PACS number(s): 42.65.Tg, 42.50.Gy, 78.67.De

I. INTRODUCTION

Solitons refer to a special kind of waves that can propagate undistorted over a long distance and remain unaffected after the collision with each other. Solitons have been observed in many fields of physics [1–10], such as optical fibers [2] and cold-atom media [3–9]. Solitons in the optical domain are of special interests because of their potential applications in the information processing and communication. On the other hand, optical transitions between electronic states within the conduction bands of semiconductor quantum wells have proved to be a promising candidate for the realization of optical devices and solid quantum information sciences [11], and large number of efforts has been devoted to the investigations of both linear and nonlinear optical properties in quantum wells.

Due to strong electron-electron interactions, the two-dimensional electron gas behaves effectively as a single oscillator, with atomiclike intersubband transition (ISBT) responses [11]. In these solid-state systems, the large intrinsic dipole matrix elements may give rise to a fast Rabi oscillation in the time domain, which allow coherent processes to occur on the time scales shorter than the typical ISBT dipole dephasing time. Moreover, the ISBT energies and electron wave-function symmetries can be engineered. Due to this unique flexibility, which can be hardly found in other systems, a large number of theoretical schemes have been proposed and some experimental realizations have been reported, such as gain without inversion [12–15], coherently controlled photocurrent generation [16], electromagnetically induced transparency [17], slow light [18], quantum interference and coherence [19–22], optical bistability [23], and solitons [24]. More recently, we have also studied the slow optical soliton formations based on the Fano interference with a three-level system of electronic subbands in an asymmetric double quantum well (GaAs/AlGaAs) structure, in which the interference between the absorption paths through two resonances to the continuum leads to a linear rapidly varying refractive index change with a reduction in the group velocity [25].

In the soliton community, it is well known that soliton management plays a crucial role in the control of their dynamics and interactions [26]. During the past 10 years, there have been intensive developments in the soliton management, such as the dispersion management in optical fiber solitons to suppress the Gordon-Haus effect [27,28], the nonlinear management to provide the compensation of the nonlinear phase shift in soliton fiber lasers [29], and the Feshbach-resonance management to stabilize matter-wave solitons in Bose-Einstein condensates [30]. Here due to the unique flexibility of coupled quantum wells, we present a totally different soliton management scheme, coined as *detuning management*, in our proposed soliton systems by changing the one- and two-photon detuning frequencies with a given function of time. In our scheme, we can easily demonstrate that the bright soliton can evolve into a dark soliton by adiabatically changing the one- and two-photon detunings Δ_1 and Δ_2 . In fact, these two detunings can vary in a wide range, which in experiments can be controlled by adjusting the height or width of the barrier through the bias voltage [31].

This work is organized as follows. We first show the existence of optical solitons based on bound-to-bound ISBT in an asymmetric three-coupled quantum well (TCQW) structure. For this purpose, we consider a four-subband cascade configuration by applying a pulsed probe field and two continuous wave (cw) control laser fields and demonstrate both analytically and numerically that optical solitons can be indeed formed in this TCQW system under appropriate conditions. The formation of optical solitons is mainly a result of the balance between the Kerr nonlinearity induced by the two cw control fields and the dispersion of our proposed system. Subsequently, we study the stability of solitons and show that a robust recovery of shapes occurs after solitons collision. To further confirm the optical soliton obtained and check their stability, we also perform additional numerical simulations starting directly from the density-matrix method without using any approximation. With controllable resonance frequencies, we present the concept of detuning management for optical solitons in coupled quantum wells. Unlike other soliton managements, such as those in optical fibers and ultracold atomic systems, the adiabatic condition to evolve a bright optical soliton into a dark one is given. We

*wenxingyang2@126.com

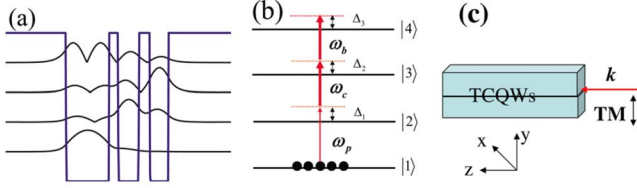


FIG. 1. (Color online) (a) Conduction-band energy diagrams for a single period of the three-coupled quantum well nonlinear optical structure. The GaInAs wells have thicknesses of 42, 20, and 18 Å (from left to right), respectively, and are separated by a 16 Å AlInAs barrier. The dashed curves represent the corresponding wave functions. (b) Schematic of the energy-level arrangement for the quantum wells under the consideration here. Subband levels are labeled as $|1\rangle$, $|2\rangle$, $|3\rangle$, and $|4\rangle$, respectively. The subband transition $|1\rangle \leftrightarrow |2\rangle$ is driven by a weak probe field with the half Rabi frequency Ω_p , while the subband transitions $|2\rangle \leftrightarrow |3\rangle$ and $|3\rangle \leftrightarrow |4\rangle$ are coupled by two control fields with the half Rabi frequencies Ω_c and Ω_b , respectively. (c) Possible launching geometry. Lights are injected with the wave vectors k ($k_{p,b,c}$) parallel to the plane of the TCQW (z axis) and y direction denotes the growth axis. The polarization state of the field (TM) is also indicated. This configuration is preferred due to a relatively long propagation distance, on the order of millimeters, to observe the soliton formation.

also show that in our TCQW scheme the carrier frequencies are adjustable in the ranges of the terahertz frequencies, which should be important for chemical detections and biological and medical imaging applications.

II. MASTER EQUATIONS AND LINEAR DYNAMICS OF THE MODEL

We consider an asymmetric semiconductor quantum well structure with four energy levels that forms the well-known cascade configuration [11,32], as shown in Fig. 1, where all possible transitions are dipole allowed. ω_{21} , ω_{32} , and ω_{43} present the energy differences of $|1\rangle \leftrightarrow |2\rangle$, $|2\rangle \leftrightarrow |3\rangle$, and $|3\rangle \leftrightarrow |4\rangle$, respectively. Such structures have been already studied for high-order nonlinear optical properties [32]. As an example, our TCQW samples can consist of 40 coupled-well periods with the material Al_{0.48}In_{0.52}As/Ga_{0.47}In_{0.53}As grown by the molecular-beam epitaxy lattice matched to a semi-insulating (100) InP substrate and separated from each other by a 150-Å undoped AlInAs barrier. Only the thickest wells are n -type doped with silicon in the structures ($1 \times 10^{18} \text{ cm}^{-3}$). Undoped 100-Å GaInAs spacer layers separate the multiquantum well structure from n^+ 4000-Å-thick GaInAs contact layers. The layer thicknesses can be verified by a transmission electron microscopy. Compared with AlGaAs/GaAs quantum well structures, our structure has a number of advantages for which concerns the physics of intersubband transitions: (i) the effective mass in the barrier material (AlInAs) is significantly smaller than that in the high Al concentration compositions of AlGaAs. The latter one is required to confine four equally spaced bound states, so that the coupling barrier does not need to be problematically thin (<10 Å) and (ii) the electron effective mass in GaInAs has the advantage of larger dipole matrix elements

for the same intersubband transition energies. The sample considered here can be designed to have the energy levels as $\epsilon_1=151$ meV, $\epsilon_2=270$ meV, $\epsilon_3=386$ meV, and $\epsilon_4=506$ meV, respectively [33]. As shown in Fig. 1(c), all the lights propagate along the z axis (parallel to the plane of the TCQW) within our TCQW sample, and we consider a transverse magnetically (TM) polarized probe field incident with respect to the growth direction (y axis). This configuration is preferred due to a relatively long propagation distance, on the order of millimeters, to observe the soliton formation. The electric field of the system can be written as

$$\vec{E} = \vec{e}_p E_p \exp(-i\omega_p t + i\vec{k}_p \cdot \vec{r}) + \vec{e}_c E_c \exp(-i\omega_c t + i\vec{k}_c \cdot \vec{r}) + \vec{e}_b E_b \exp(-i\omega_b t + i\vec{k}_b \cdot \vec{r}) + \text{c.c.},$$

where \vec{e}_j and \vec{k}_j are the related unit vector of the field and the wave vector with the slowly varying envelope E_j , respectively.

In the present analysis we assume that the semiconductor quantum wells with low dopings are designed such that electron-electron effects have very small influences in our results. Many-body effects (for example, the depolarization effect, which renormalizes the free-carrier and carrier-field contributions) are not included in our study [34]. In Schrödinger's picture with the rotating-wave approximation, the semiclassical Hamiltonian describing the system under study can be written as

$$H = \sum_{j=2}^4 \epsilon_j |j\rangle \langle j| - \hbar(\Omega_c e^{-i\omega_c t}|3\rangle \langle 2| + \Omega_b e^{-i\omega_b t}|4\rangle \langle 3| + \Omega_p e^{-i\omega_p t}|2\rangle \langle 1| + \text{H.c.}), \quad (1)$$

where $\Omega_p = (\vec{\mu}_{12} \cdot \vec{e}_p) E_p / \hbar$, $\Omega_c = (\vec{\mu}_{23} \cdot \vec{e}_c) E_c / \hbar$, and $\Omega_b = (\vec{\mu}_{34} \cdot \vec{e}_b) E_b / \hbar$ are the corresponding half Rabi frequencies with $\vec{\mu}_{ij}$ being the dipole moment for the relevant intersubband transition. For simplicity, we have taken ϵ_1 for the ground-state level $|1\rangle$ as the energy origin. Turning to the interaction picture, the above Hamiltonian can be rewritten as follows:

$$\frac{H_0}{\hbar} = \omega_p |2\rangle \langle 2| + (\omega_p + \omega_c) |3\rangle \langle 3| + (\omega_p + \omega_c + \omega_b) |4\rangle \langle 4|, \quad (2)$$

$$\frac{H_I}{\hbar} = -\Delta_1 |2\rangle \langle 2| - \Delta_2 |3\rangle \langle 3| - \Delta_3 |4\rangle \langle 4| - (\Omega_c |3\rangle \langle 2| + \Omega_b |4\rangle \langle 3| + \Omega_p |2\rangle \langle 1| + \text{H.c.}), \quad (3)$$

where the ISBT detunings of three optical fields are defined by $\Delta_1 = \omega_p - \epsilon_2 / \hbar$ (single-photon detuning), $\Delta_2 = \omega_p + \omega_c - \epsilon_3 / \hbar$ (two-photon detuning), and $\Delta_3 = \omega_p + \omega_c + \omega_b - \epsilon_4 / \hbar$ (three-photon detuning), respectively. The density-matrix equations of motion for the system can be written as follows:

$$\dot{\rho}_{11} = i\Omega_p^* \rho_{21} - i\Omega_p \rho_{12}, \quad (4)$$

$$\dot{\rho}_{22} = -\gamma_2 \rho_{22} + i\Omega_p \rho_{12} + i\Omega_c^* \rho_{32} - i\Omega_p^* \rho_{21} - i\Omega_c \rho_{23}, \quad (5)$$

$$\dot{\rho}_{33} = -\gamma_3 \rho_{33} + i\Omega_c \rho_{23} + i\Omega_b^* \rho_{43} - i\Omega_c^* \rho_{32} - i\Omega_b \rho_{34}, \quad (6)$$

$$\dot{\rho}_{44} = -\gamma_4 \rho_{44} + i\Omega_b \rho_{34} - i\Omega_b^* \rho_{43}, \quad (7)$$

$$\dot{\rho}_{21} = id_{21} \rho_{21} + i\Omega_p (\rho_{11} - \rho_{22}) + i\Omega_c^* \rho_{31}, \quad (8)$$

$$\dot{\rho}_{31} = id_{31} \rho_{31} + i\Omega_c \rho_{21} + i\Omega_b^* \rho_{41} - i\Omega_p \rho_{32}, \quad (9)$$

$$\dot{\rho}_{41} = id_{41} \rho_{41} + i\Omega_b \rho_{31} - i\Omega_p \rho_{42}, \quad (10)$$

$$\dot{\rho}_{32} = id_{32} \rho_{32} + i\Omega_c (\rho_{22} - \rho_{33}) + i\Omega_b^* \rho_{42} - i\Omega_p^* \rho_{31}, \quad (11)$$

$$\dot{\rho}_{42} = id_{42} \rho_{42} + i\Omega_b \rho_{32} - i\Omega_c \rho_{43} - i\Omega_p^* \rho_{41}, \quad (12)$$

$$\dot{\rho}_{43} = id_{43} \rho_{43} + i\Omega_b (\rho_{33} - \rho_{44}) - i\Omega_c^* \rho_{42} \quad (13)$$

with $d_{21} = \Delta_1 + i\gamma_{21}$, $d_{31} = \Delta_2 + i\gamma_{31}$, $d_{41} = \Delta_3 + i\gamma_{41}$, $d_{32} = \Delta_2 - \Delta_1 + i\gamma_{32}$, $d_{42} = \Delta_3 - \Delta_1 + i\gamma_{42}$, $d_{43} = \Delta_3 - \Delta_2 + i\gamma_{43}$, and $\rho_{nm} = \rho_{mn}^*$. Actually, these density-matrix equations (4)–(13) are to be supplemented by the population conservation condition $\rho_{11} + \rho_{22} + \rho_{33} + \rho_{44} = 1$. The decay and dephasing rates are included phenomenologically in the above equations. The population scattering rates γ_i are primarily due to the longitudinal optical-phonon emission events at low temperature [35,36]. The total dephasing rates γ_{ij} ($i \neq j$) are given by $\gamma_{21} = (\gamma_2 + \gamma_{21}^{dph})/2$, $\gamma_{32} = (\gamma_2 + \gamma_3 + \gamma_{32}^{dph})/2$, $\gamma_{31} = (\gamma_3 + \gamma_{31}^{dph})/2$, $\gamma_{41} = (\gamma_4 + \gamma_{41}^{dph})/2$, $\gamma_{42} = (\gamma_2 + \gamma_4 + \gamma_{42}^{dph})/2$, and $\gamma_{43} = (\gamma_3 + \gamma_4 + \gamma_{43}^{dph})/2$, where the pure dipole dephasing rates γ_{ij}^{dph} are assumed to be a combination of quasielastic interface roughness scattering or acoustic-phonon scattering [15,21,37]. A comprehensive treatment of the decay rates would involve incorporation of the decay mechanisms into the Hamiltonian of the system. However, we have adopted the phenomenological approach of treating the decay mechanisms just as done in the literature. [14,19–23,25,37,38]. A more fully two-dimensional treatment taking into account of these processes has been investigated quite thoroughly by some authors (see, for example, [17,24,39,40]).

The electric-field evolution is governed by the Maxwell equation

$$\nabla^2 \vec{E} - \frac{1}{c^2} \frac{\partial^2 \vec{E}}{\partial t^2} = \frac{1}{\epsilon_0 c^2} \frac{\partial^2 \vec{P}}{\partial t^2} \quad (14)$$

with

$$\begin{aligned} \vec{P} = & N \{ \vec{\mu}_{12} \rho_{21} \exp[i(\vec{k}_p \cdot \vec{r} - \omega_p t)] + \vec{\mu}_{23} \rho_{32} \exp[i(\vec{k}_c \cdot \vec{r} - \omega_c t)] \\ & + \vec{\mu}_{34} \rho_{43} \exp[i(\vec{k}_b \cdot \vec{r} - \omega_b t)] + \text{c.c.} \}, \end{aligned} \quad (15)$$

where N , c , and ϵ_0 being the concentration, velocity of light in vacuum, and vacuum dielectric constant, respectively. Under the slowly varying envelope approximation [41], the Maxwell equation can be reduced to the first-order equation. Thus we can obtain the slowly varying envelope equation for describing the probe field evolution, i.e.,

$$\frac{\partial \Omega_p(z,t)}{\partial z} + \frac{1}{c} \frac{\partial \Omega_p(z,t)}{\partial t} = i\kappa \rho_{21}, \quad (16)$$

where $\kappa = N\Omega_p |\vec{e}_p \cdot \vec{\mu}_{12}|^2 / (2\epsilon_0 \hbar c)$. For simplicity, we have assumed $\vec{k}_p = \vec{e}_z k_p$.

Before solving the nonlinear coupled equations (4)–(13) and (16), let us first examine the linear excitations of the system, which may provide useful hints of the weak nonlinear theory developed in the following. We assume that the half Rabi frequency Ω_p of probe field is much smaller than that of the control fields $\Omega_{c,b}$, so that the initial population in the ground state $|1\rangle$ are not depleted; therefore, $\rho_{11} \approx 1$ while $\rho_{22} \approx \rho_{33} \approx \rho_{44} \approx 0$. Then under the perturbation expansion $\rho_{ij} = \sum_k \rho_{ij}^{(k)}$, where $\rho_{ij}^{(k)}$ is the k th-order part of ρ_{ij} in terms of Ω_p , it can be shown that $\rho_{ij}^{(0)} = 0$ ($i \neq j$) and $\rho_{22}^{(k)} = \rho_{33}^{(k)} = \rho_{44}^{(k)} = 0$. Considering the first order of the pulsed probe field and taking time Fourier transform of Eqs. (8)–(13) and (16),

$$\rho_{jk}^{(1)}(t) = \frac{1}{\sqrt{2\pi}} \int_{-\infty}^{\infty} \beta_{jk}^{(1)}(\omega) \exp(-i\omega t) d\omega, \quad j,k = 1,2,3,4, \quad (17)$$

$$\Omega_p(t) = \frac{1}{\sqrt{2\pi}} \int_{-\infty}^{\infty} \Lambda_p(\omega) \exp(-i\omega t) d\omega \quad (18)$$

with ω being the Fourier-transform variable, we have

$$(\omega + d_{21}) \beta_{21}^{(1)} + \Lambda_p + \Omega_c^* \beta_{31}^{(1)} = 0, \quad (19)$$

$$(\omega + d_{31}) \beta_{31}^{(1)} + \Omega_c \beta_{21}^{(1)} + \Omega_b^* \beta_{41}^{(1)} - \Lambda_p \beta_{32}^{(0)} = 0, \quad (20)$$

$$(\omega + d_{41}) \beta_{41}^{(1)} + \Omega_b \beta_{31}^{(1)} - \Lambda_p \beta_{42}^{(0)} = 0, \quad (21)$$

$$(\omega + d_{32}) \beta_{32}^{(1)} + \Omega_b^* \beta_{42}^{(1)} - \Lambda_p^* \beta_{31}^{(0)} = 0, \quad (22)$$

$$(\omega + d_{42}) \beta_{42}^{(1)} + \Omega_b \beta_{32}^{(1)} - \Omega_c \beta_{43}^{(1)} - \Lambda_p^* \beta_{41}^{(0)} = 0, \quad (23)$$

$$(\omega + d_{43}) \beta_{43}^{(1)} - \Omega_c^* \beta_{42}^{(1)} = 0, \quad (24)$$

and

$$\frac{\partial \Lambda_p}{\partial z} - i \frac{\omega}{c} \Lambda_p = i\kappa \beta_{21}^{(1)}. \quad (25)$$

With the help of Eqs. (19)–(24), Eq. (25) can be solved analytically, yielding

$$\Lambda_p(z, \omega) = \Lambda_p(0, \omega) \exp[iK(\omega)z], \quad (26)$$

where $K(\omega)$ is the linear dispersion relation for the probe field. In typical operation conditions $K(\omega)$ can be expanded into a rapidly converging power series around the center frequency ω_p of the weak probe field, i.e., $\omega=0$. We thus have

$$K(\omega) = \frac{\omega}{c} + \kappa \frac{D_p(\omega)}{D(\omega)} = K_0 + K_1 \omega + K_2 \omega^2 + O(\omega^3) \quad (27)$$

with $D_p(\omega) = (\omega + d_{31})(\omega + d_{41}) - |\Omega_b|^2$ and $D(\omega) = |\Omega_c|^2(\omega + d_{31}) + |\Omega_b|^2(\omega + d_{21}) - (\omega + d_{21})(\omega + d_{31})(\omega + d_{41})$. The physical interpretation of the dispersion coefficient in Eq. (25) is clear. $K_0 = \phi + i\alpha/2$ describes the linear absorption coefficient α and the phase shift ϕ per unit length of the probe field. $K_1 = dK(\omega)/d\omega|_{\omega=0}$ gives the propagation group velocity and $K_2 = d^2 K(\omega)/d\omega^2|_{\omega=0}$ represents the group-velocity dispersion that contributes to the shape change and additional loss

of field intensity. We note that there exist parameter regimes in which the absorptions of the probe field can be significantly suppressed due to the interference produced from the contribution of two control fields by choosing appropriate conditions in the present system.

It should be noted that Eq. (25) is obtained in the linear regime of the system under the weak-field and adiabatic approximations by ignoring higher-order terms of the probe field. In order to preserve the shape of probe field, we need to include the self-phase modulation (SPM) effect which may balance the spread effect due to the group-velocity dispersion (describing by the K_2 coefficient). In Sec. III, we will explore the higher-order terms of Ω_p with systematically keeping terms up to ω^2 in Eq. (27) for the purpose of demonstrating the formation of temporal optical solitons in our TCQW system.

III. NONLINEAR DYNAMICS AND OPTICAL SOLITONS

With the dispersion coefficients obtained, we now investigate the nonlinear evolution of the probe field. We first show that it is indeed possible to obtain a set of rather clean and reasonable parameters that will lead to the formation of optical solitons. By substituting a trial function $\Lambda(z, \omega) = \Lambda(z, \omega)\exp(iK_0z)$ into the wave equation (25), we obtain

$$\frac{\partial \Lambda(z, \omega)}{\partial z} e^{iK_0z} = i[K_1\omega + K_2\omega^2]\Lambda(z, \omega)e^{iK_0z}. \quad (28)$$

Here we only keep terms up to the order ω^2 in expanding the propagation constant $K(\omega)$. In order to balance the interplay between group-velocity dispersion and nonlinear effect, it is necessary for us to consider the nonlinear polarization on the right-hand sides of Eq. (16),

$$K_2 = -\frac{2D_p(0)[C + (d_{21} + d_{31} + d_{41})D(0)] + C(d_{31} + d_{41})D(0) + D(0)^2}{D(0)^3}, \quad (35)$$

where $D_p(0) = d_{31}d_{41} - |\Omega_b|^2$ and $C = |\Omega_b|^2 + |\Omega_c|^2 - d_{21}d_{31} - d_{21}d_{41} - d_{31}d_{41}$. Equation (33) has complex coefficients and in general does not allow soliton solutions. However, as we show below, if a reasonable and realistic set of parameters can be found so that $\exp(-\alpha l) \approx 1$, i.e., the losses of the probe pulse are small enough to be neglected, then the balance between the nonlinear SPM and the group-velocity dispersion may sustain a pulse with a shape-invariant propagation, which yields $K_2 = K_{2r} + iK_{2i} \approx K_{2r}$ and $W = W_r + iW_i \approx W_r$. By defining $\xi = z/(2L_D)$ and $\eta = (t-z/V_g)/\tau_0$, then Eq. (33) can be rewritten in the dimensionless form corresponding to the standard nonlinear Schrödinger equation governing the pulsed probe field evolution,

$$i\frac{\partial u}{\partial \xi} + \frac{\partial^2 u}{\partial \eta^2} + 2u|u|^2 = 0, \quad (36)$$

where $u = \Omega_p/U_0$, $L_D = \tau_0^2/|K_{2r}|$ is the characteristic dispersion length, and $L_{NL} = 1/(U_0^2 W_r)$ is the nonlinear length. In Eq.

$$i\kappa\rho_{21} \approx i\kappa\rho_{21}^{(1)} + iNLT, \quad (29)$$

where the nonlinear term “NLT” is denoted by $NLT = -\kappa\rho_{21}^{(1)}e^{-iK_0z}(|\rho_{21}^{(1)}|^2 + |\rho_{31}^{(1)}|^2 + |\rho_{41}^{(1)}|^2)$ and $\rho_{21}^{(1)}$, $\rho_{31}^{(1)}$, and $\rho_{41}^{(1)}$ can be obtained by solving Eqs. (19)–(24), i.e.,

$$\rho_{21}^{(1)} = \frac{d_{31}d_{41} - |\Omega_b|^2}{D(0)}\Omega_p, \quad (30)$$

$$\rho_{31}^{(1)} = \frac{d_{41}\Omega_c}{D(0)}\Omega_p, \quad (31)$$

$$\rho_{41}^{(1)} = \frac{\Omega_b\Omega_c}{D(0)}\Omega_p \quad (32)$$

with $D(0) = |\Omega_c|^2 d_{31} + |\Omega_b|^2 d_{21} - d_{21}d_{31}d_{41}$. With the help of nonlinear polarization term, we now turn to the investigation of the nonlinear dynamics in the present system. Taking the inverse Fourier transformation of Eq. (28), we can have the nonlinear wave equation for the slow varying envelope $\Omega_p(z, t)$,

$$i\frac{\partial \Omega_p(z, t)}{\partial z} - \frac{K_2}{2}\frac{\partial^2 \Omega_p(z, t)}{\partial t^2} - W \exp[-\alpha z]|\Omega_p(z, t)|^2\Omega_p(z, t) = 0, \quad (33)$$

where absorption coefficients $\alpha = 2 \operatorname{Im}(K_0)$. The coefficients K_2 and W characterize the group-velocity dispersion and the nonlinearity of probe field, respectively, with the formalisms given by

$$W = \frac{\kappa D_p(0)[|D_p(0)|^2 + |\Omega_c|^2(|\Omega_b|^2 + \Delta_3^2 + \gamma_4^2)]}{D(0)|D(0)|^2}, \quad (34)$$

(36) we have assumed that the characteristic dispersion length L_D is equal to the characteristic nonlinear length L_{NL} of the system and $U_0 = (1/\tau_0)[|K_{2r}|/W_r]^{1/2}$ is the typical Rabi frequency of the probe field. Equation (36) supports the exact bright soliton solutions as

$$u = 2\beta \operatorname{sech}[2\beta(\eta - \eta_0 + 4\delta\xi)]e^{-2i\delta\eta - 4i(\beta^2 - \beta^2)\xi} \quad (37)$$

with β , δ , and η_0 being real parameters which determine the amplitude, propagating velocity, and initial position of the soliton, respectively. By taking $\beta = 1/2$ and $\delta = \eta_0 = \phi_0 = 0$, Eq. (37) can be reduced to $u = \operatorname{sech}(\eta)\exp(i\xi)$ or, in terms of the probe field,

$$\Omega_p = U_0 \operatorname{sech}[(t - z/V_g)/\tau_0]e^{iz/(2L_D)}. \quad (38)$$

In fact, Eq. (37) admits solutions of bright and dark solitons depending on the sign of the product $K_{2r}W_r$ [42]. The single soliton solution (38) is called as the fundamental soliton and N soliton ($N=2, 3, \dots$) is named as the higher-order soliton

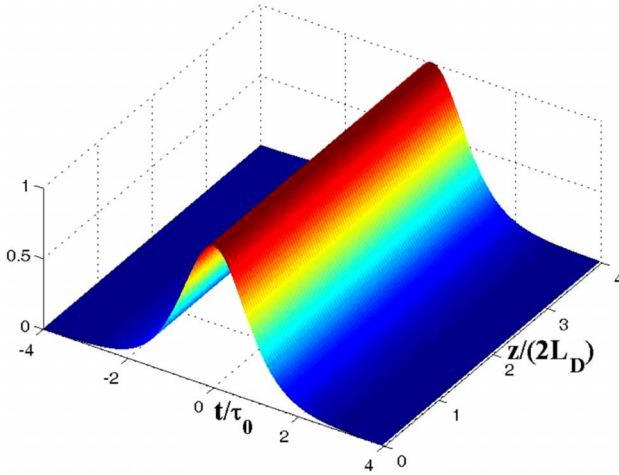


FIG. 2. (Color online) Surface plot of the probe intensity $|\Omega_p/U_0|^2$ versus dimensionless time t/τ_0 and distance $z/(2L_D)$ obtained by numerically solving Eq. (33) without neglecting the imaginary part of coefficients with the initial condition given in Eq. (38).

(breathers). After returning to original variables, the bright two-soliton (bright soliton of second order) solution of Eq. (36) reads

$$\Omega_p = U_0 \frac{4[\cosh(3\eta) + 3 \exp(8iz/L_D)\cosh(\eta)]\exp(iz/L_D)}{\cosh(4\eta) + 4 \cosh(2\eta) + 3 \cos(8z/L_D)}. \quad (39)$$

Checking our assumption that leads to Eqs. (33)–(36) is indeed practical. Below we give a practical example for a realistic TCQW system, with the population scattering rates

$\gamma_2=\gamma_3=\gamma_4=0.24 \text{ ps}^{-1}$ and the total dephasing rates $\gamma_{21}=4.8 \text{ ps}^{-1}$, $\gamma_{31}=\gamma_{32}=1.9 \text{ ps}^{-1}$, and $\gamma_{41}=\gamma_{42}=\gamma_{43}=1.4 \text{ ps}^{-1}$ (all the decay rates are estimated from Refs. [11,32]). Besides, taking $\Omega_b=\Omega_c=2 \text{ ps}^{-1}$, $\Delta_1=-3.5 \text{ ps}^{-1}$, $\Delta_2=-6 \text{ ps}^{-1}$, $\Delta_3=8 \text{ ps}^{-1}$, $\tau_0=300 \text{ fs}$, and $\kappa=2.4 \text{ ps}^{-1} \mu\text{m}^{-1}$, we have $K_2=(-1.54-0.075i)\times 10^{-26} \mu\text{m}^{-1} \text{s}^2$ and $W=(-1.17+0.069i)\times 10^{-24} \mu\text{m}^{-1} \text{s}^2$. Clearly, for all complex coefficients the imaginary parts are indeed much smaller than their corresponding real parts. At the same time, we obtain $\alpha=0.0036 \mu\text{m}^{-1}$, $L_D=L_{NL}=5.8 \mu\text{m}$, and $U_0=0.38 \text{ ps}^{-1}$. With these parameters, the standard nonlinear Schrödinger equation in Eq. (36) with $K_{2r}W_r>0$ is well characterized, and hence the existence of bright solitons in the TCQW structures is supported. In Fig. 2, we show the result of numerical simulation on the soliton wave shape $|\Omega_p/U_0|$ versus dimensionless time t/τ_0 and distance $z/(2L_D)$ with the full complex coefficients by taking Eq. (38) as an initial condition. One can find that in this case the soliton is fairly stable during propagation, which is mainly produced from the balance between dispersion and nonlinearity. Thus the result of numerical simulation shows excellent agreement with the exact soliton solution in Eq. (38). We also show that a particular interesting phenomenon in Fig. 3 about the bright two-soliton solution. We see that a bright two-soliton solution can survive even with a certain small attenuation.

The collision property between two solitons is one of the most intriguing aspects in soliton dynamics. By using numerical simulations we have also investigated the collision feature between two bright optical solitons in the present TCQW system. Figure 4 shows the wave forms for two different solitons, in which one soliton is obtained by taking $\beta=0.3$, $\delta=0$, and $\sigma_0=1.0$, whereas the other is obtained by taking $\beta=0.4$, $\delta=-0.2$, and $\sigma_0=-2.0$ in Eq. (37). One can find that both solitons have resumed their original shapes

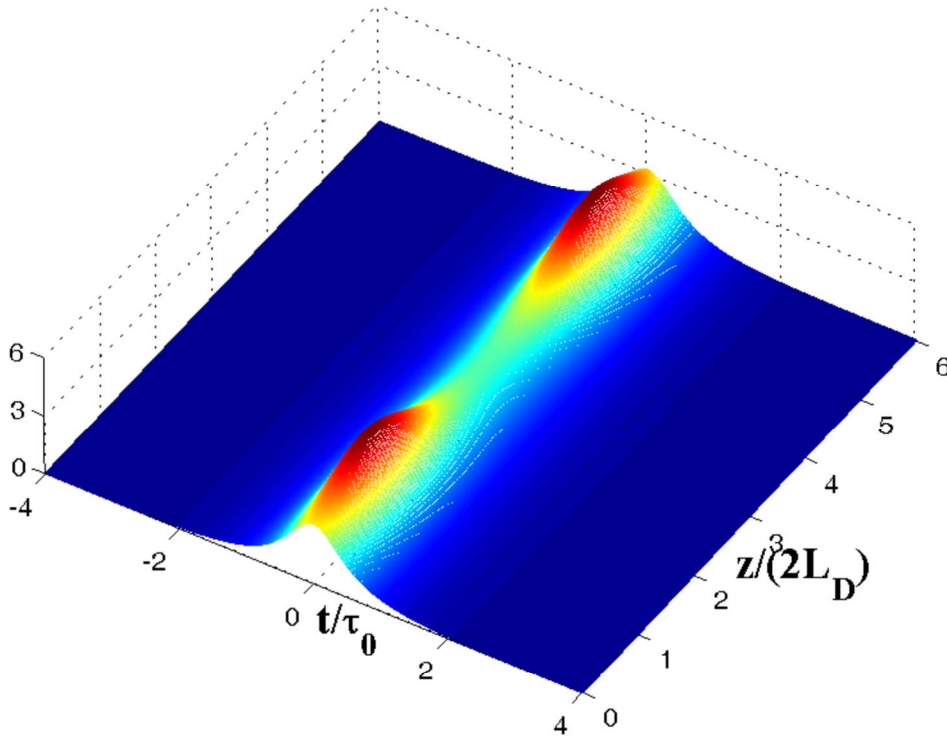


FIG. 3. (Color online) Surface plot of the probe intensity $|\Omega_p/U_0|^2$ versus dimensionless time t/τ_0 and distance $z/(2L_D)$ obtained by numerically solving Eq. (33) without neglecting the imaginary part of coefficients with the initial condition given in Eq. (39). Here, we have chosen the same parameters as in Fig. 2.

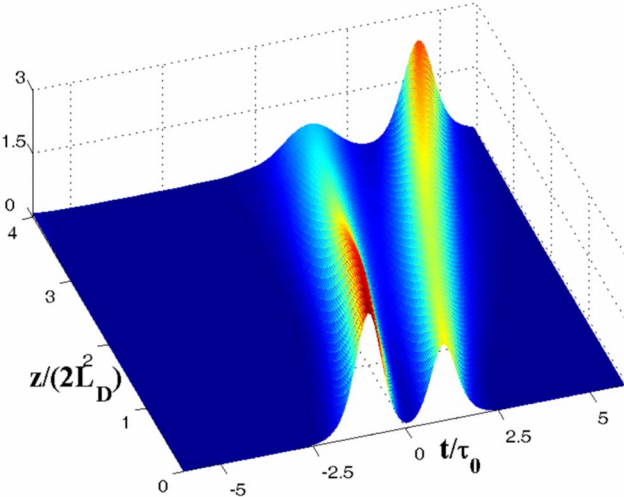


FIG. 4. (Color online) Surface plot of the solitary wave intensity $|\Omega_p/U_0|^2$ versus dimensionless time t/τ_0 and distance $z/(2L_D)$ for the collision between two solitons by solving Eq. (33). The initial condition is given in the main text and other parameters are the same as in Fig. 2.

after the collision, indicating that the optical solitons produced in the present system are stable during the collision. More interestingly, as the chosen different phase (position), a repulsive or absorptive interaction can be realized in the collision [1,2], leading to a modulation or switching in a Mach-Zehnder configuration when the phase-shifted soliton interferes with another reference soliton [43]. Thus we may provide more practical opportunities to implement all-optical switching and electro-optical modulated solid-state devices due to the flexibility in the semiconductor quantum structures.

To make a further confirmation on the optical soliton solutions obtained above and check their stability, we also perform additional numerical simulations starting directly from

Eqs. (4)–(13) and (16) without using any approximation. Figure 5(a) is the propagation of $z=8 \mu\text{m}$ for the probe field intensity $|\Omega_p/U_0|^2$, with Eq. (38) as the input condition. One can find that, except for small ripples appearing on its peak due to higher-order dispersions and higher-order nonlinear effects that have not been included, the optical solitons produced here is rather stable as expected. We also show in Fig. 5(b) the simulation result of the collision between two bright optical solitons with the same initial condition as in Fig. 4. One can see again that the result is in a great agreement with the results shown in Fig. 4, and thus the full model in Eqs. (4)–(13) and (16) supports nearly shape-preserving soliton propagation.

IV. ADIABATIC CONDITIONS FOR THE DETUNING MANAGEMENT

In the following, we consider the case of dark solitons. We take $\Delta_1=3.5 \text{ ps}^{-1}$ and $\Delta_2=6 \text{ ps}^{-1}$, along with all other parameters given above unchanged. In this case we obtain $\alpha=0.0036 \mu\text{m}^{-1}$, $K_2=(1.63-0.026i)\times 10^{-26} \mu\text{m}^{-1}\text{s}^2$, and $W=(-1.21-0.068i)\times 10^{-24} \mu\text{m}^{-1}\text{s}^2$. With these parameters, one has the product $K_{2r}W_r<0$. Hence we can obtain dark solitons that travel in the TCQW system. With the original variable, the fundamental dark soliton solution of Eq. (36) is given by

$$\Omega_p = U_0 \tanh[(t-z/V_g)/\tau_0] e^{iz/(2L_D)}, \quad (40)$$

where the amplitude U_0 and width τ_0 are arbitrary constants and subjected only to the constraint $|U_0\tau|^2=|K_{2r}|/W_r$ (or $L_D=L_{NL}$). This indicates again that the formation of the optical solitons given above is due to the balance between the group-velocity dispersion and nonlinearity (i.e., SPM effect). Equation (40) gives the so-called “black” dark soliton [42]. Compared to the bright solitons, here we only need to change the one- and two-photon detunings in the proposed TCQW structure for dark soliton solutions.

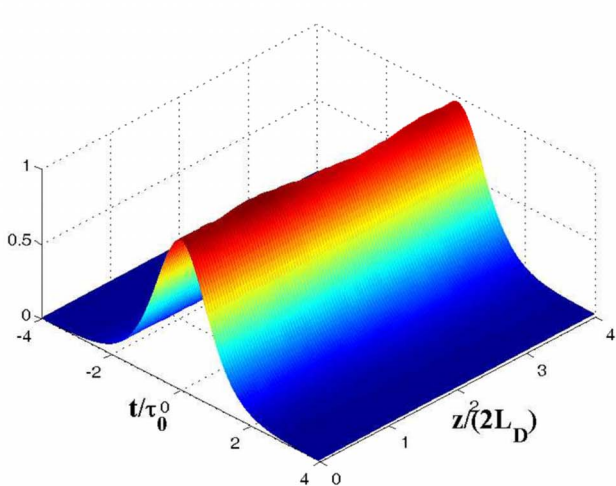
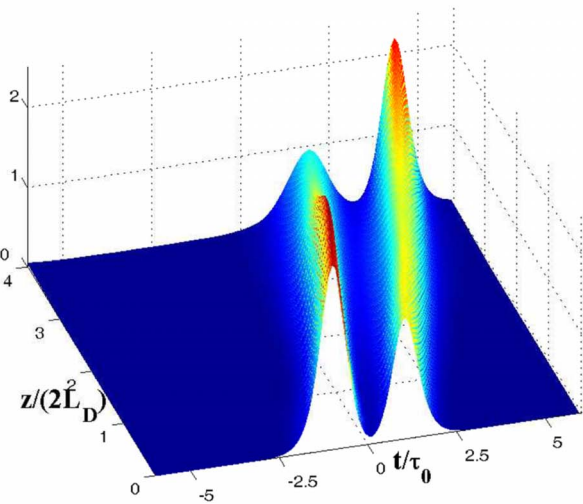


FIG. 5. (Color online) (a) Surface plot of the solitary wave intensity $|\Omega_p/U_0|^2$ versus dimensionless time t/τ_0 and distance $z/(2L_D)$ for the collision between two solitons by numerically integrating Eqs. (4)–(13) and (16) with the initial condition given in Eq. (38). (b) Collision between two solitons and other parameters are the same as in Fig. 3.



In the fiber optic telecommunications, dispersion management is introduced by applying a long fiber link consisting of periodically alternating segments of fibers with opposite signs of the group-velocity dispersions [26]. Here with the existences of optical bright and dark solitons and the unique tunability in our proposed TCQW structure, one can vary the corresponding resonance conditions of input optical fields by a given specific time-dependent function for the detuning frequencies. As a simple example, we shall demonstrate the evolution from a bright soliton into a dark one by adiabatically changing the one- and two-photon detunings Δ_1 and Δ_2 . This interesting result is produced from that the signs of the dispersion and nonlinear coefficients are dependent upon the signs of one- and two-photon detunings, which can provide another soliton management scheme for another possible soliton switching (bright \leftrightarrow dark). Without loss of generality, we suppose the parameters change as a function of the time t , i.e.,

$$\Delta_1(t) = \Delta_1^{(0)} + b_1 t, \quad (41)$$

$$\Delta_2(t) = \Delta_2^{(0)} + b_2 t, \quad (42)$$

where $\Delta_1^{(0)} = -3.5 \text{ ps}^{-1}$ and $\Delta_2^{(0)} = -6 \text{ ps}^{-1}$. b_1 and b_2 are assumed to be positive constants. When the detuning Δ_1 varies from -3.5 to 3.5 ps^{-1} and Δ_2 varies from -6 to 6 ps^{-1} , which can be realized by changing the energy levels of the quantum well through the applied bias voltage, the evolution of the bright soliton to the dark soliton is achieved. The adiabatic condition required for such a simple detuning management is

$$\left| \frac{\langle n | \frac{\partial}{\partial t} | m \rangle}{E_n - E_m} \right| \ll 1 \quad (43)$$

for $n \neq m$. It is easy to testify that

$$\langle n | \frac{\partial}{\partial t} | m \rangle = \frac{\langle n | \partial H_{\text{QW}}(t) / \partial t | m \rangle}{E_m - E_n}, \quad (44)$$

where $H_{\text{QW}} = \sum_{j=2}^4 E_j |j\rangle \langle j|$ is the Hamiltonian of quantum well. For our scheme, from Eqs. (41) and (42), we obtain the adiabatic condition as follows:

$$\sqrt{b_1}, \sqrt{b_2} \ll \frac{|E_i - E_j|}{\hbar} \quad (45)$$

for $i, j = 1, 2, 3$ and $i \neq j$. This adiabatic condition implies that the change rate for the corresponding eigenenergy in our quantum wells should be slow enough to not raise the transition between different states. Like dispersion-managed systems, in our proposed TCQW structure various detuning management schemes should also have a strong impact on the stability and noise of optical solitons. But here we only give the necessary condition to perform such a totally different soliton management.

V. DISCUSSION AND CONCLUSION

Before conclusion, we give a brief discussion on the required threshold optical power density to support stable soliton propagation [44]. In the parameter regime for the fundamental bright soliton discussed above, the flux of energy of the probe optical field associated with a single soliton is given by the Poynting vector integrated over the cross section of the quantum well sample: $P = \int dS (\vec{E}_p \times \vec{H}_p) \cdot \vec{e}_z$, where \vec{e}_z is the unit vector in the propagation direction. Assuming that the polarized direction of the probe field is unchanged, we have $\vec{E}_p = (E_p, 0, 0)$ and $\vec{H}_p = (0, H_p, 0)$, where $H_p = \epsilon_0 c n_p E_p$ with $n_p = 1 + c \operatorname{Re}(K)/\omega_p$ being the refractive index of the probe field. Note that $E_p = (\hbar/|\mu_{12}|)\Omega_p \exp[i(\omega_{pz}/c - \omega_{pt})] + \text{c.c.}$, then we can obtain the average flux of the probe field energy over the carrier-wave period as

$$\bar{P} = \frac{2\epsilon_0 c n_p S_0 (\hbar/|\mu_{12}|)^2 K_{2r}}{\tau_0^2 W_r} \operatorname{sech}^2[(t - z/v_g)/\tau_0], \quad (46)$$

where the first term $2\epsilon_0 c n_p S_0 (\hbar/|\mu_{12}|)^2 K_{2r} / \tau_0^2 W_r$ in Eq. (46) is the peak power, with S_0 being the cross-section area of the probe laser beam. We can see that the peak power is directly proportional to the dispersion coefficient K_{2r} and inversely proportional to the square of the pulse width τ_0 as well as the SPM coefficient W_r . Using the parameters in our numerical simulations for the fundamental bright soliton and taking $S_0 = \pi \times 10^{-4} \text{ cm}^2$, we found that the required peak power is about 37 mW. Thus we argue that very low input power is needed for generating optical solitons using our proposed TCQW system.

In addition, with the parameters provided there, the dispersion length of our system is about $L_D = 5.8 \text{ } \mu\text{m}$, which is long enough for the observation of optical solitons with our proposed coupled geometry as shown in Fig. 1(c). It is worth to point out that there are some relevant works on optical solitons and optical breathers in semiconductor devices. For example in Ref. [45], Adamashvili *et al.* considered the condition of self-induced transparency (SIT) in multilevel quantum dots, in which a single optical field with 2π or 0π area is needed to induce the required coherent pulse propagation, while here we use three input optical fields, i.e., two cw control and one probe fields, which construct the quantum interference channels and lead to a giant suppression of the linear absorption and simultaneously an enhancement of SPM coefficient for the probe field. Besides, our proposed cascade quantum structure supports stable soliton propagation not only on the nanoscales but also at very low input light power levels.

In conclusion, we have shown that it is possible to support a stable propagation of optical solitons by using the density-matrix equations in a four-level cascade electronic subband system. We also demonstrated that under realistic physical conditions stable optical solitons can form and propagate undistorted in our TCQW system. With the well-known flexibilities in solid-state systems, we also present the concept of detuning management scheme for optical solitons in quantum wells. We analyze the adiabatic condition to perform such another soliton management and demonstrate the evolution from a bright soliton into a dark one. Besides, the

carrier frequencies of the solitons obtained here are on the order of $\omega_{21} = (\epsilon_2 - \epsilon_1)/\hbar \sim 28$ THz. If one applied the different electric bias voltage (for example, -20 kV/cm) to the structure, the transition frequency between the bands 2 and 1 can be changed to about 21 THz [32]. In other words, the carrier frequencies of the bright and dark solitons are adjustable via varying the external bias voltage within the terahertz frequency regimes, which should be useful to the community of terahertz technologies.

ACKNOWLEDGMENTS

The research was supported in part by National Natural Science Foundation of China under Grants No. 10704017 and No. 10874050, by National Fundamental Research Program of China under Grant No. 2005CB724508, and by the National Science Council of Taiwan with Contracts No. NSC 95-2112-M-007-058-MY3 and No. NSC 95-2120-M-001-006.

-
- [1] Yu. S. Kivshar and G. P. Agrawal, *Optical Solitons: From Fibers to Photonic Crystals* (Academic, San Diego, 2003).
- [2] G. P. Agrawal, *Nonlinear Fiber Optics*, 3rd ed. (Academic, New York, 2001); A. Hasegawa and M. Matsumoto, *Optical Solitons in Fibers* (Springer, Berlin, 2003).
- [3] R. K. Lee, Elena A. Ostrovskaya, Y. S. Kivshar, and Y. Lai, Phys. Rev. A **72**, 033607 (2005).
- [4] Y. Wu and L. Deng, Phys. Rev. Lett. **93**, 143904 (2004).
- [5] X. T. Xie, W. B. Li, and W. X. Yang, J. Phys. B **39**, 401 (2006).
- [6] Y. Wu and L. Deng, Opt. Lett. **29**, 2064 (2004).
- [7] X. J. Liu, H. Jing, and M. L. Ge, Phys. Rev. A **70**, 055802 (2004).
- [8] Y. Wu, Phys. Rev. A **71**, 053820 (2005).
- [9] L. Deng, M. G. Payne, G. Huang, and E. W. Hagley, Phys. Rev. E **72** 055601(R) (2005).
- [10] D. V. Skryabin, A. V. Yulin, and A. I. Maimistov, Phys. Rev. Lett. **96**, 163904 (2006).
- [11] H. C. Liu and F. Capasso, *Intersubband Transitions in Quantum Wells: Physics and Device Applications* (Academic, New York, 2000).
- [12] A. Imamoglu and R. J. Ram, Opt. Lett. **19**, 1744 (1994).
- [13] J. Faist, F. Capasso, C. Sirtori, K. West, and L. N. Pfeiffer, Nature (London) **390**, 589 (1997).
- [14] C. R. Lee, Y. C. Li, F. K. Men, C. H. Pao, Y. C. Tsai, and J. F. Wang, Appl. Phys. Lett. **86**, 201112 (2005).
- [15] M. D. Frogley, J. F. Dynes, M. Beck, J. Faist, and C. C. Phillips, Nature Mater. **5**, 175 (2006).
- [16] R. Atanasov, A. Hache, J. L. P. Hughes, H. M. van Driel, and J. E. Sipe, Phys. Rev. Lett. **76**, 1703 (1996).
- [17] L. Silvestri, F. Bassani, G. Czajkowski, and B. Davoudi, Eur. Phys. J. B **27**, 89 (2002).
- [18] P. C. Ku, F. Sedgwick, C. J. Chang-Hasnain, P. Palinginis, T. Li, H. Wang, S. W. Chang, and S. L. Chuang, Opt. Lett. **29**, 2291 (2004).
- [19] J. Faist, C. Sirtori, F. Capasso, S. N. G. Chu, L. N. Pfeiffer, and K. W. West, Opt. Lett. **21**, 985 (1996).
- [20] G. B. Serapiglia, E. Paspalakis, C. Sirtori, K. L. Vodopyanov, and C. C. Phillips, Phys. Rev. Lett. **84**, 1019 (2000).
- [21] E. Paspalakis, M. Tsousidou, and A. F. Terzis, Phys. Rev. B **73**, 125344 (2006).
- [22] P. I. Tamborenea and H. Metiu, Phys. Lett. A **240**, 265 (1998).
- [23] J. H. Li, Phys. Rev. B **75**, 155329 (2007).
- [24] F. Biancalana, S. B. Healy, R. Fehse, and E. P. O'Reilly, Phys. Rev. A **73**, 063826 (2006).
- [25] W. X. Yang, J. M. Hou, and R.-K. Lee, Phys. Rev. A **77**, 033838 (2008).
- [26] B. A. Malomed, *Soliton Management in Periodic Systems* (Springer, New York, 2006), and references therein.
- [27] F. M. Knox, W. Forsyak, and N. J. Doran, J. Lightwave Technol. **13**, 1955 (1995).
- [28] M. Nakazawa and H. Kubota, Electron. Lett. **31**, 216 (1995).
- [29] X. Liu, L. Qian, and F. Wise, Opt. Lett. **24**, 1777 (1999).
- [30] P. G. Kevrekidis, G. Theocharis, D. J. Frantzeskakis, and B. A. Malomed, Phys. Rev. Lett. **90**, 230401 (2003).
- [31] J. Faist, F. Capasso, C. Sirtori, D. L. Sivco, A. L. Hutchinson, S. N. G. Chu, and A. Y. Cho, Appl. Phys. Lett. **65**, 94 (1994).
- [32] C. Sirtori, F. Capasso, J. Faist, and S. Scandolo, Phys. Rev. B **50**, 8663 (1994).
- [33] Following a common usage in semiconductor physics [11], times are here given in units of the Planck constant \hbar , so that the energy of 1 meV ($\hbar\nu = \hbar/\tau = 10^{-3}$ eV) corresponds to a time $\tau = (\hbar)\cdot 10^{-3}$ eV $^{-1} \approx 4.1$ ps. Likewise for frequencies, the energy of 1 meV corresponds to a frequency of 242 GHz.
- [34] D. E. Nikonorov, A. Imamoglu, L. V. Butov, and H. Schmidt, Phys. Rev. Lett. **79**, 4633 (1997).
- [35] P. I. Tamborenea and H. Metiu, J. Chem. Phys. **110**, 9202 (1999).
- [36] S. M. Goodnick and P. Lugli, in *Hot Carriers in Semiconductor Nanostructures*, edited by J. Shah (Academic, New York, 1992), Chap. 3, p. 219.
- [37] W. Potz, Phys. Rev. B **71**, 125331 (2005).
- [38] J. H. Wu, J. Y. Gao, J. H. Xu, L. Silvestri, M. Artoni, G. C. La Rocca, and F. Bassani, Phys. Rev. Lett. **95**, 057401 (2005).
- [39] I. Waldmüller, J. Förstner, S.-C. Lee, A. Knorr, M. Woerner, K. Reimann, R. A. Kaindl, T. Elsaesser, R. Hey, and K. H. Ploog, Phys. Rev. B **69**, 205307 (2004).
- [40] T. Shih, K. Reimann, M. Woerner, T. Elsaesser, I. Waldmüller, A. Knorr, R. Hey, and K. H. Ploog, Phys. Rev. B **72**, 195338 (2005).
- [41] M. O. Scully and M. S. Zubairy, *Quantum Optics* (Cambridge University Press, Cambridge, England, 1997), Chap. 5, p. 168.
- [42] Yu. S. Kivshar and B. Luther-Davies, Phys. Rep. **298**, 81 (1998).
- [43] S. R. Friberg, Opt. Lett. **16**, 1484 (1991).
- [44] Y. Wu and P. T. Leung, Phys. Rev. A **60**, 630 (1999).
- [45] G. T. Adamashvili, C. Weber, A. Knorr, and N. T. Adamashvili, Phys. Rev. A **75**, 063808 (2007).